

# Concentration Profiles of Individual Species in Coupled Binding of Two Ligands by a Receptor

Isard Dunietz, Irving M. Klotz,\* and Joseph A. Walder

Integrated DNA Technologies, Inc., 8930 Gross Point Road, Skokie, Illinois 60077

Received: February 12, 2003; In Final Form: July 13, 2003

Equations for the concentration profiles of all species in equilibria in the coupled binding of two ligands to a receptor have been formulated in a compact translucent form convenient for numerical analyses. These have been used to generate graphical presentations of the variation of each profile over a wide range of ligand concentration. New insights into the distribution of species have been obtained.

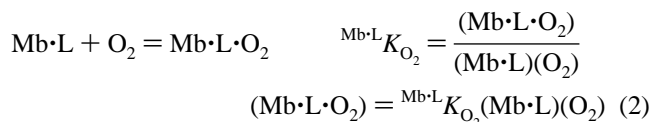
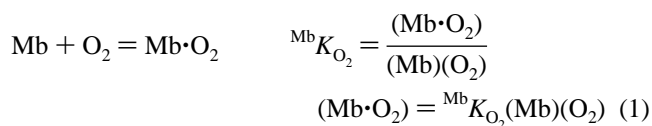
It has been evident since Gibbs<sup>1</sup> formulation of the foundations of chemical thermodynamics that in solution, the behavior of each component is coupled to that of the other ones. That constraint is usually expressed in terms of the chemical potentials,  $\mu_i$ , in the format of the Gibbs–Duhem equation. In protein–ligand interactions such a linkage was demonstrated early by Bohr<sup>2</sup> a century ago in studies of the effects of  $H^+$  ion on uptake of  $O_2$  by hemoglobin. Subsequently, Wyman<sup>3,4</sup> formulated general thermodynamic relationships for the binding by a receptor of coupled ligands.

It is usually difficult to visualize the concentration profiles of individual ligands in such systems from the thermodynamic equations governing their interactions. Such profiles could provide fresh insights into the redistribution of equilibria between species as ligand concentration is varied.

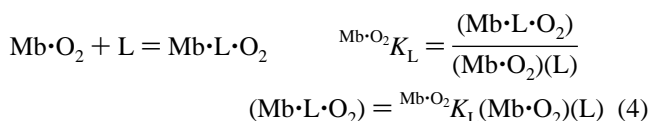
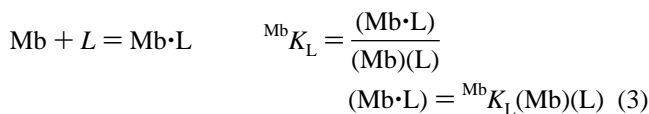
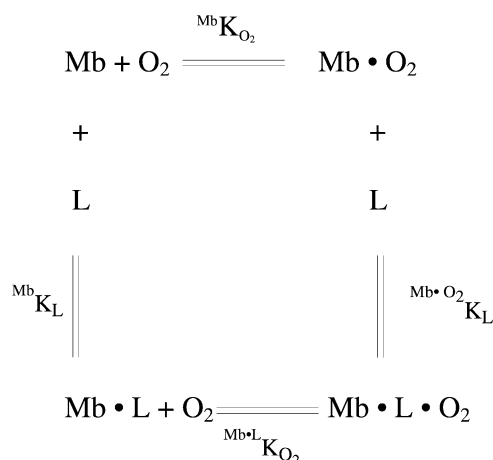
## Delineation of Coupled Equilibria

The format of our analysis will be illustrated with a minimal coupled system, a receptor that can bind each of two ligands with unit stoichiometry for each species. For didactic purposes we have visualized a concrete example of such a system, the binding by myoglobin of  $O_2$  and of a ligand L (which does not ligate to the heme iron).

Schematically, we can represent the coupled binding of the two ligands by the diagram in Scheme 1. Specifically the equilibria and the corresponding stoichiometric<sup>5</sup> equilibrium constants are defined by the following equations:



## SCHEME 1



For convenience in later algebraic manipulations, we also define the coupling parameter:

$$\lambda \equiv \frac{{}^{Mb \cdot L}K_{O_2}}{{}^{Mb}K_{O_2}} = \frac{{}^{Mb \cdot O_2}K_L}{{}^{Mb}K_L} \quad (5)$$

The second equality follows from the thermodynamic constraint

$${}^{Mb}K_{O_2} {}^{Mb \cdot O_2}K_L = {}^{Mb}K_L {}^{Mb \cdot L}K_{O_2} \quad (6)$$

## Expressions for Species Concentrations

For the total molar concentration of myoglobin ( $c_T$ ) we write

$$c_T \equiv (Mb) + (Mb \cdot L) + (Mb \cdot O_2) + (Mb \cdot L \cdot O_2) \quad (7)$$

Keeping eqs 1–4 in mind, we can convert eq 7 into

\* Corresponding author: Department of Chemistry, Northwestern University, 2145 N. Sheridan Road, Evanston, IL 60208-3113. Telephone: (847) 491-3546. Fax: (847) 491-7713.

$$c_T = (\text{Mb})[1 + (\text{L})^{\text{Mb}}K_L + (\text{O}_2)^{\text{Mb}}K_{\text{O}_2} + \lambda(\text{O}_2)^{\text{Mb}}K_{\text{O}_2}(\text{L})^{\text{Mb}}K_L] \quad (8)$$

Then we express the fractional concentration of (Mb),  $f_{\text{Mb}}$  as

$$f_{\text{Mb}} = \frac{(\text{Mb})}{c_T} = \frac{1}{1 + (\text{L})^{\text{Mb}}K_L + (\text{O}_2)^{\text{Mb}}K_{\text{O}_2} + \lambda(\text{O}_2)^{\text{Mb}}K_{\text{O}_2}(\text{L})^{\text{Mb}}K_L} \quad (9)$$

For the other myoglobin species, the respective fractional concentrations are

$$f_{\text{Mb}\cdot\text{L}} = \frac{(\text{Mb}\cdot\text{L})}{c_T} = (\text{L})^{\text{Mb}}K_L f_{\text{Mb}} \quad (10)$$

$$f_{\text{Mb}\cdot\text{O}_2} = \frac{(\text{Mb}\cdot\text{O}_2)}{c_T} = (\text{O}_2)^{\text{Mb}}K_{\text{O}_2} f_{\text{Mb}} \quad (11)$$

$$f_{\text{Mb}\cdot\text{L}\cdot\text{O}_2} = \frac{(\text{Mb}\cdot\text{L}\cdot\text{O}_2)}{c_T} = \lambda(\text{O}_2)^{\text{Mb}}K_{\text{O}_2}(\text{L})^{\text{Mb}}K_L f_{\text{Mb}} \quad (12)$$

For numerical computations, the following compact display is expedient:

$$(\text{Mb}):(\text{Mb}\cdot\text{L}):(\text{Mb}\cdot\text{O}_2):(\text{Mb}\cdot\text{L}\cdot\text{O}_2) = 1:(\text{L})^{\text{Mb}}K_L:(\text{O}_2)^{\text{Mb}}K_{\text{O}_2}:\lambda(\text{O}_2)^{\text{Mb}}K_{\text{O}_2}(\text{L})^{\text{Mb}}K_L \quad (13)$$

### Analytical Equations for Graphical Presentations

For myoglobin–oxygen equilibria, a reasonable choice<sup>6</sup> for  $^{\text{Mb}}K_{\text{O}_2}$  is 0.72 Torr<sup>−1</sup>. For illustrative calculations, we choose a convenient low oxygen pressure so that

$$(\text{O}_2)^{\text{Mb}}K_{\text{O}_2} = \frac{1}{2} \quad (14)$$

Let us examine first the concentration profiles for

$$\lambda = 10^5 \quad (15)$$

i.e., when the affinity of Mb for L is very much weaker than that of Mb·O<sub>2</sub> and the affinity of Mb for O<sub>2</sub> is much weaker than that of Mb·L (see eq 5).

At very low concentrations of L, i.e., as (L) → 0, there is essentially no L bound to Mb or Mb·O<sub>2</sub>, so

$$f_{\text{Mb}\cdot\text{L}} \approx 0$$

$$f_{\text{Mb}\cdot\text{L}\cdot\text{O}_2} \approx 0$$

Nevertheless, we can see from eq 13

$$\frac{(\text{Mb}\cdot\text{O}_2)}{(\text{Mb})} = \frac{(\text{O}_2)^{\text{Mb}}K_{\text{O}_2}}{1} = \frac{1}{2} \quad (16)$$

or

$$(\text{Mb}):(\text{Mb}\cdot\text{O}_2) = 2:1 \quad (17)$$

This behavior is visible (Figure 1) throughout the concentration range of (L), actually presented as a dimensionless, normalized ligand concentration

$$\xi \equiv (\text{L})^{\text{Mb}}K_L$$

in the graph. For convenience in computation, we have set  $^{\text{Mb}}K_L = 1 \text{ M}^{-1}$  throughout this paper so that  $\xi = (\text{L})$ .

With increasing ligand concentration, the species Mb·L and Mb·L·O<sub>2</sub> begin to appear, the latter in larger concentration because  $^{\text{Mb}\cdot\text{O}_2}K_L$  is much greater than  $^{\text{Mb}}K_L$  (the assumed value of  $\lambda$  being 10<sup>5</sup>). As  $(\text{L})^{\text{Mb}}K_L \rightarrow \infty$ , the nonligated species, Mb and Mb·O<sub>2</sub> become vanishingly small, so  $c_T$  is constituted of Mb·L and Mb·L·O<sub>2</sub> as always at relative concentrations given by

$$\frac{(\text{Mb}\cdot\text{L}\cdot\text{O}_2)}{(\text{Mb}\cdot\text{L})} = \lambda(\text{O}_2)^{\text{Mb}}K_{\text{O}_2} \quad (18)$$

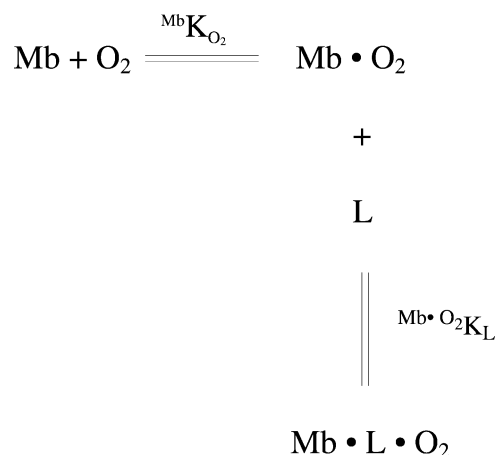
(which follows from eq 13). Keeping eq 14 in mind, we see that the product on the right side of eq 18 must always be 0.5 × 10<sup>5</sup>. The respective profiles are presented individually in Figure 1. Because the chosen value of  $\lambda$  is 10<sup>5</sup>, the scale of the ordinate axis for  $f_{\text{Mb}\cdot\text{L}}$  has to be greatly expanded, and  $f_{\text{Mb}\cdot\text{L}}$  is always tiny.

As (L) approaches 10<sup>−5</sup> M,  $f_{\text{Mb}}$ ,  $f_{\text{Mb}\cdot\text{O}_2}$ , and  $f_{\text{Mb}\cdot\text{L}\cdot\text{O}_2}$  are each appreciable. As (L) is increased further, Mb·L·O<sub>2</sub> becomes the dominant species. Nevertheless, Mb is in equilibrium with Mb·O<sub>2</sub>, at relative concentrations of 2:1 (see eq 17). At high concentrations, (L) ≫ 10<sup>−5</sup> M,  $f_{\text{Mb}}$ ,  $f_{\text{Mb}\cdot\text{L}}$ , and  $f_{\text{Mb}\cdot\text{O}_2}$  are all negligible. Furthermore, because  $^{\text{Mb}}K_L$  and  $^{\text{Mb}}K_{\text{O}_2}$  are small compared to  $^{\text{Mb}\cdot\text{O}_2}K_L$  and  $^{\text{Mb}\cdot\text{L}}K_{\text{O}_2}$ , respectively, Mb·O<sub>2</sub> is increasingly depleted as it is progressively converted into Mb·L·O<sub>2</sub>. Nevertheless, the ratio

$$(\text{Mb})/(\text{Mb}\cdot\text{O}_2) = 2$$

must be maintained. The net result is to reduce Scheme 1 to Scheme 2.

### SCHEME 2



In Figure 2, the individual profiles in Figure 1 have been assembled together into a graph with a single set of coordinate axes, with the abscissa spanning the range of ligand concentrations of 10<sup>−10</sup> < (L) < 10<sup>2</sup> M. It is clear that the oxygenated species dominate the assembly, except at very low (L) < 10<sup>−5</sup> M. In contrast, the fraction  $f_{\text{Mb}\cdot\text{L}}$  is too small,  $f_{\text{Mb}\cdot\text{L}} \leq 2 \times 10^{-5}$ , to be visible.

With the illustrations of Figures 1 and 2, we can now explore the effects of changes in the value of the coupling parameter  $\lambda$  (eq 5) on the concentration profiles. We have examined 10<sup>5</sup>, 10<sup>3</sup>, 10<sup>1</sup>, 10<sup>0</sup>, 10<sup>−1</sup>, 10<sup>−3</sup>, and 10<sup>−5</sup>.

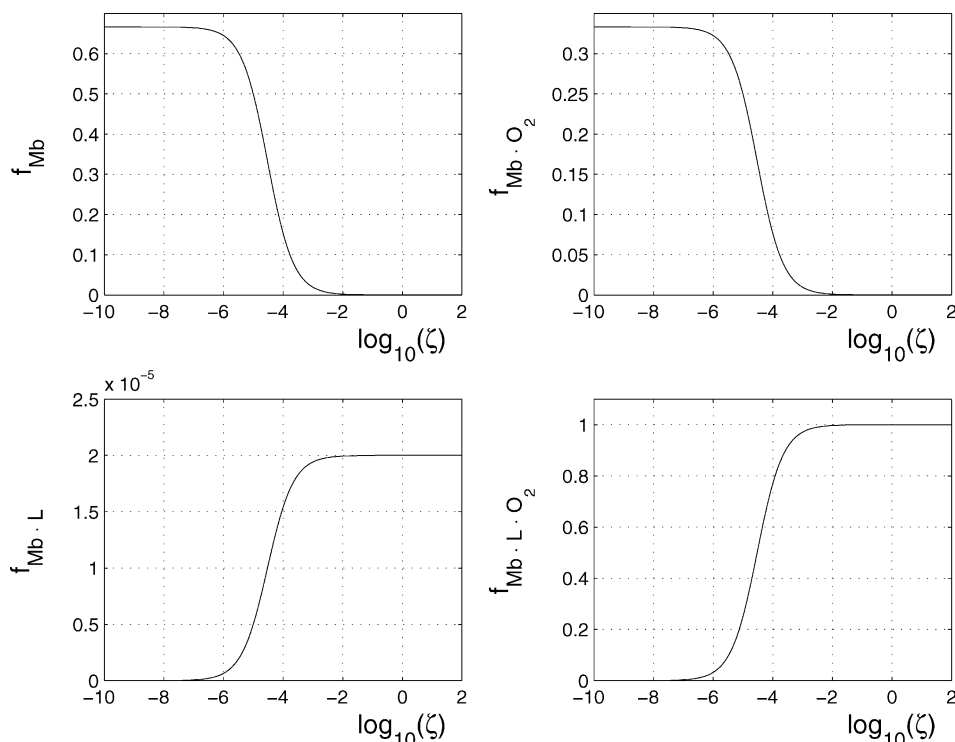


**Figure 1.** Concentration profiles for Mb, Mb·O<sub>2</sub>, Mb·L, and Mb·L·O<sub>2</sub> respectively, presented on individual coordinate scales. The normalized ligand concentration is  $\zeta \equiv (L)^{Mb}K_L$  (dimensionless). Governing parameters:  $^{Mb}K_{O_2}(O_2) = 0.5$ ,  $\lambda = 10^5$ .

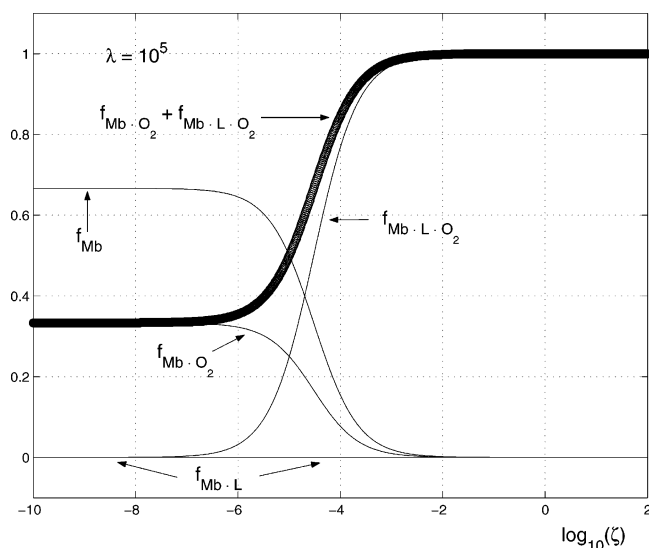


**Figure 2.** Concentration profiles compared in a graph with a single set of coordinate axes. Governing parameters:  $^{Mb}K_{O_2}(O_2) = 0.5$ ,  $\lambda = 10^5$ . With this ordinate scale, the profile for  $f_{Mb \cdot L}$  is not visible because it hugs the abscissa axis over the entire range of  $\zeta \equiv (L)^{Mb}K_L$  (dimensionless).

In each case, we start with eq 13, the master relationship linking the individual species concentrations.

It is of interest to focus first on  $\lambda = 10^0 = 1$ , the pivot point in the series. When  $\lambda = 1$ ,

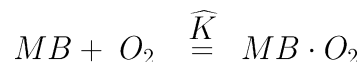
$$^{Mb \cdot L}K_{O_2} = ^{Mb}K_{O_2}$$

$$^{Mb \cdot O_2}K_L = ^{Mb}K_L$$

that is, the affinity of Mb·L for O<sub>2</sub> is identical with that of Mb, and the affinity of Mb·O<sub>2</sub> for L is the same as that of Mb. Turning to Scheme 1, we see that these relations mean that the

bottom horizontal equation cannot be distinguished thermodynamically from the top one, so the two can be collapsed into one, Scheme 3,

### SCHEME 3



in which

$$(MB) = (Mb) + (Mb \cdot L) \quad (19)$$

$$(MB \cdot O_2) = (Mb \cdot O_2) + (Mb \cdot L \cdot O_2) \quad (20)$$

Phenomenologically Mb and Mb·L are indistinguishable and Mb·O<sub>2</sub> and Mb·L·O<sub>2</sub> are indistinguishable, so only one oxygenation equilibrium is evident experimentally; that is, the observed equilibrium constant is independent of (L).

The master relationship, eq 13, verifies the qualitative arguments for the case of  $\lambda = 1$ . From eq 13 it follows that

$$\frac{(Mb)}{(Mb \cdot L)} = \frac{1}{(L)^{Mb}K_L} = \frac{(Mb \cdot O_2)}{(Mb \cdot L \cdot O_2)} \quad (21)$$

or

$$\frac{(Mb)}{(Mb \cdot O_2)} = \frac{1}{(O_2)^{Mb}K_{O_2}} = \frac{(Mb \cdot L)}{(Mb \cdot L \cdot O_2)} \quad (22)$$

Table 1 presents the relative magnitudes of each of the individual species, governed by the master eq 13, for a full range of values of  $\lambda$  from  $10^5$  to  $10^{-5}$ . For each  $\lambda$ , the species concentrations have been explored over a range of concentration of (L) from  $10^{-4}$  to  $10^4$ . The table summarizes the changes in relative species concentration in a compact form.

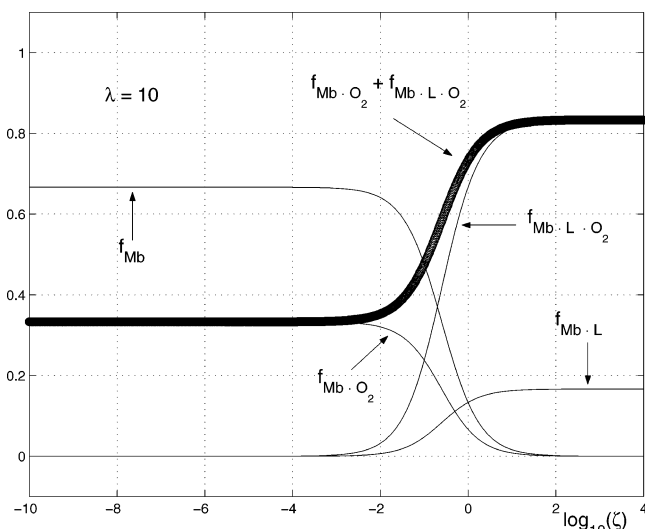
Graphs of the full concentration profiles have also been prepared. Only two additional ones are presented here.<sup>7</sup>

Figure 3 displays profiles when the coupling parameter is

**TABLE 1: Variation of Relative Concentrations of Myoglobin–Ligand Species with Change of Ligand Coupling Parameter  $\lambda^a$** 

$\zeta \equiv (L)^{Mb}K_L$	$\lambda$	(Mb)	(Mb·L)	(Mb·O <sub>2</sub> )	(Mb·L·O <sub>2</sub> )
$10^{-4}$	$10^5$	1	$10^{-4}$	0.5	5
$10^{-4}$	$10^3$	1	$10^{-4}$	0.5	$5 \times 10^{-2}$
$10^{-4}$	$10^1$	1	$10^{-4}$	0.5	$5 \times 10^{-4}$
$10^{-4}$	1	1	$10^{-4}$	0.5	$5 \times 10^{-5}$
$10^{-4}$	$10^{-1}$	1	$10^{-4}$	0.5	$5 \times 10^{-6}$
$10^{-4}$	$10^{-3}$	1	$10^{-4}$	0.5	$5 \times 10^{-8}$
$10^{-4}$	$10^{-5}$	1	$10^{-4}$	0.5	$5 \times 10^{-10}$
1	$10^5$	1	1	0.5	$5 \times 10^4$
1	$10^3$	1	1	0.5	$5 \times 10^2$
1	$10^1$	1	1	0.5	5
1	1	1	1	0.5	$5 \times 10^{-1}$
1	$10^{-1}$	1	1	0.5	$5 \times 10^{-2}$
1	$10^{-3}$	1	1	0.5	$5 \times 10^{-4}$
1	$10^{-5}$	1	1	0.5	$5 \times 10^{-6}$
$10^4$	$10^5$	1	$10^4$	0.5	$5 \times 10^8$
$10^4$	$10^3$	1	$10^4$	0.5	$5 \times 10^6$
$10^4$	$10^1$	1	$10^4$	0.5	$5 \times 10^4$
$10^4$	1	1	$10^4$	0.5	$5 \times 10^3$
$10^4$	$10^{-1}$	1	$10^4$	0.5	$5 \times 10^2$
$10^4$	$10^{-3}$	1	$10^4$	0.5	5
$10^4$	$10^{-5}$	1	$10^4$	0.5	$5 \times 10^{-2}$

<sup>a</sup> (O<sub>2</sub>)<sup>Mb</sup>K<sub>O<sub>2</sub></sub> set at 0.5 throughout these computations.

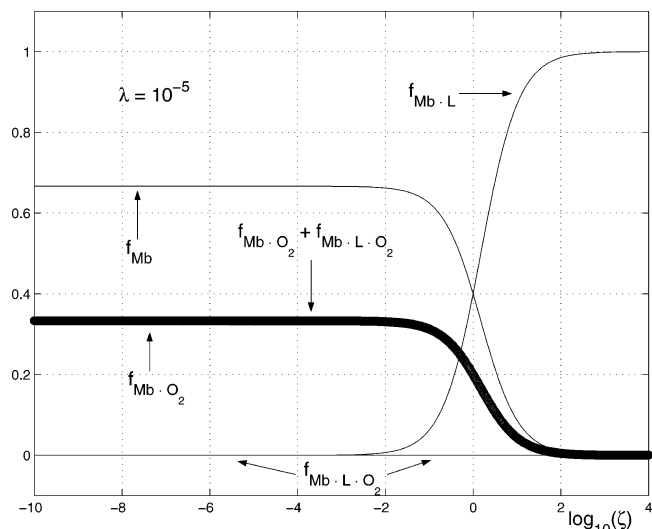
**Figure 3.** Concentration profiles when coupling of ligands is weaker. Governing parameters: <sup>Mb</sup>K<sub>O<sub>2</sub></sub>(O<sub>2</sub>) = 0.5,  $\lambda = 10$ ,  $\zeta \equiv (L)^{Mb}K_L$  (dimensionless).

10, instead of  $10^5$ . The primary differences from Figure 2 are the following. In general, the curves are shifted to much higher concentrations of ligand L. For the fraction oxygenated, the inflection point is shifted from (L) of about  $10^{-5}$  to about  $10^{-1}$ . Similarly,  $f_{Mb·L}$  is shifted markedly to higher (L) concentrations, and its magnitude is increased enormously, so that it is very visible (at (L) =  $10^{-2}$  to  $10^4$  M), whereas when  $\lambda = 10^5$  (Figure 2)  $f_{Mb·L}$  is so small that it is invisible compared to the other species.

It is also of interest to examine the effect of an inverted magnitude of  $\lambda$ . Figure 4 presents concentration profiles for  $\lambda = 10^{-5}$ . Most striking is the turnaround in general course of the curve for fraction oxygenated; with increasing (L) it moves toward zero, whereas for  $\lambda = 10^5$ , its asymptote is 1. Furthermore, Mb·L now appears visible at (L)  $\approx 10^{-2}$  M and becomes the dominant species at (L)  $\sim 1$  M.

### Partition of Ligand L Between Deoxymyoglobin and Oxy-myoglobin

To explore this distribution quantitatively, we define the following quantities:

**Figure 4.** Concentration profiles when reversed coupling is strengthened. Governing parameters: <sup>Mb</sup>K<sub>O<sub>2</sub></sub>(O<sub>2</sub>) = 0.5,  $\lambda = 10^{-5}$ ,  $\zeta \equiv (L)^{Mb}K_L$  (dimensionless).

$$f_L^{Mb} \equiv \frac{(Mb \cdot L)}{(Mb) + (Mb \cdot L)} \quad (23)$$

$$f_L^{Mb \cdot O_2} \equiv \frac{(Mb \cdot O_2 \cdot L)}{(Mb \cdot O_2) + (Mb \cdot O_2 \cdot L)} \quad (24)$$

$$\nu \equiv f_L^{Mb \cdot O_2} - f_L^{Mb} = \frac{\lambda \zeta}{1 + \lambda \zeta} - \frac{\zeta}{1 + \zeta} \quad (25)$$

where the final equality was obtained by inserting the master relationships (eq 13) into the definition of  $\nu$ .

For  $\lambda = 10^5$ , Figure 1 displays the concentration profiles of each of the species in eqs 23 and 24. Thus,  $\nu$  can be computed readily as a function of (L). Figure 5 includes the course of  $\nu$  for  $\lambda = 10^5$ . The quantity  $\nu$  expresses the difference in binding of L by oxygenated myoglobin as compared to deoxygenated, i.e., the left-hand side and right-hand side equilibria in Scheme 1.

One should note that  $\nu$  is independent of (O<sub>2</sub>) and of <sup>Mb</sup>K<sub>O<sub>2</sub></sub>.

Referring to Scheme 1, we can rationalize the shape of  $\nu$  – (L) curves. For  $\lambda = 10^5$ , for example, at very low concentrations of this ligand ( $< 10^{-6}$  M), neither Mb or Mb·O<sub>2</sub> will bind any L. Because  $f_L^{Mb}$  and  $f_L^{Mb \cdot O_2}$  approach zero, so does the difference  $\nu$ . At very high concentrations of L ( $> 10$  M), the equilibria in the vertical steps of Scheme 1 will be shifted increasingly downward to produce more and more Mb·L and Mb·O<sub>2</sub>·L, respectively, and simultaneously reduce the concentrations of Mb and of Mb·O<sub>2</sub> to approach zero. Consequently,  $f_L^{Mb}$  and  $f_L^{Mb \cdot O_2}$  approach 1, so their difference  $\nu$  again approaches zero. In the intermediate region, as we increase the concentration of L  $> 10^{-6}$  M, the ligand becomes increasingly bound, but primarily to Mb·O<sub>2</sub> to produce Mb·L·O<sub>2</sub> (see Scheme 1), because <sup>Mb·L</sup>K<sub>L</sub> is very much larger than <sup>Mb</sup>K<sub>L</sub> ( $\lambda = 10^5$ ). Furthermore, because <sup>Mb·L</sup>K<sub>O<sub>2</sub></sub> is very much larger than <sup>Mb</sup>K<sub>O<sub>2</sub></sub> the Mb·L that does form with increasing L is converted to Mb·L·O<sub>2</sub>. Thus the concentration of Mb·L remains very low (see Figure 1). In addition, because <sup>Mb</sup>K<sub>L</sub> is very small, (Mb·L)/(Mb) will be small (see eq 13) and  $f_L^{Mb}$  will be near zero over a wide range of (L). Consequently,  $\nu$  approaches unity over the wide intermediate range of (L); that is L is bound predominantly by Mb·O<sub>2</sub>. This plateau (Figure 5) is bordered on the left by a steep ascent, reflecting the strong binding of L

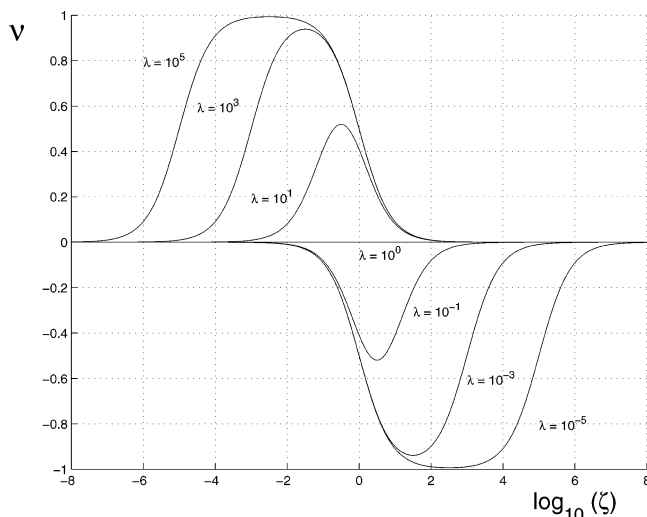


**Figure 5.** Partitioning of ligand,  $\nu$ , as a function of ligand coupling parameter,  $\lambda$ , over an extended range of normalized concentrations of ligand,  $\zeta \equiv (L)^{Mb}K_L$  (dimensionless).

by  $Mb \cdot O_2$ . The inflection point of this rise occurs at the low concentration  $(L) \sim 10^{-5}$ , consistent with the large magnitude of  $Mb \cdot O_2 K_L$ ,  $10^5 Mb K_L$  (with  $Mb K_L \equiv 1 M^{-1}$ ). Similarly, the plateau on the right is bordered by a steep decline, which reflects the binding of  $L$  by  $Mb$ . For this weak complexation one needs to attain a very high concentration of  $L$ . As Figure 5 illustrates, the inflection point of the decline of the curve for  $\lambda = 10^5$  is at  $(L) = 1$ , consistent with the small magnitude of  $Mb K_L$ .

When  $\lambda$  is decreased progressively from  $10^5$  to  $10$ , the partition curves ( $\nu$  vs  $(L)$ ) drop in maximum height and decrease in width (see Figure 5).

For values of  $\lambda$  from  $10^{-1}$  to  $10^{-5}$ , the partition curves (Figure 5) show  $\nu$  values that are always negative and are (displaced) mirror images of those for  $\lambda = 10$  to  $10^5$ . Thus a proper  $C_2$  axis perpendicular to the  $(\nu, \log_{10}(\zeta))$  plane passes through the coordinates  $(0, 0)$  in the figure. In essence,  $L$  is bound preferentially by  $Mb$  rather than by  $Mb \cdot O_2$  and hence  $\nu$  versus  $(L)$  ranges between  $-1$  and  $0$  (see eq 25).

As was pointed out earlier, when  $\lambda = 1$ , the affinity of  $Mb$  for  $L$  is the same as that of  $Mb \cdot O_2$ . Hence the partition factor of eq 23 is identical with that of eq 24, so  $\nu = 0$  throughout the entire concentration range of  $(L)$ . In Figure 5, the abscissa axis at  $\nu = 0$  is also the partition curve; i.e.,  $L$  has no preference between  $Mb$  and  $Mb \cdot O_2$ .

It is also possible to obtain  $\nu$  by an approach that does not depend on the existence of concentration profiles. If data are available for the uptake of oxygen by myoglobin at a series of concentrations of  $L$ , we can define an observed equilibrium constant  $\hat{K}$  by the equation

$$\hat{K} \equiv \frac{(Mb \cdot O_2) + (Mb \cdot L \cdot O_2)}{(Mb) + (Mb \cdot L)} \frac{1}{(O_2)} \quad (26)$$

Referring to eqs 1–4 we can obtain substitutions for  $(Mb \cdot L \cdot O_2)$  and  $(Mb \cdot L)$  so that eq 26 can be transformed into

$$\begin{aligned} \hat{K} &= \frac{(Mb \cdot O_2) + {}^{Mb \cdot O_2}K_L(Mb \cdot O_2)(L)}{(Mb) + {}^{Mb}K_L(Mb)(L)} \frac{1}{(O_2)} \\ &= \frac{(Mb \cdot O_2)}{(Mb)} \frac{1}{(O_2)} \frac{1 + {}^{Mb \cdot O_2}K_L(L)}{1 + {}^{Mb}K_L(L)} \end{aligned} \quad (27)$$

Then eq 27 can be converted to

$$\log \hat{K} = \log K_0 + \log[1 + {}^{Mb \cdot O_2}K_L(L)] - \log[1 + {}^{Mb}K_L(L)] \quad (28)$$

where  $K_0$  is the oxygenation equilibrium constant in the limit of  $(L) \rightarrow 0$ .<sup>8</sup>

From eq 3 it follows that the number of moles of  $L$  bound by deoxymyoglobin,  ${}^{Mb}B_L$ , is

$$\begin{aligned} {}^{Mb}B_L &\equiv \frac{(Mb \cdot L)}{(Mb) + (Mb \cdot L)} = \frac{{}^{Mb}K_L(Mb)(L)}{(Mb) + {}^{Mb}K_L(Mb)(L)} \\ &= \frac{{}^{Mb}K_L(L)}{1 + {}^{Mb}K_L(L)} \end{aligned} \quad (29)$$

If we represent the denominator by  $Z_{Mb}$ , then it can be shown readily<sup>5</sup> that

$${}^{Mb}B_L = \frac{d \log Z_{Mb}}{d \log(L)} \quad (30)$$

With a similar set of steps one can also prove that the number of moles of  $L$  bound by oxymyoglobin,  ${}^{Mb \cdot O_2}B_L$ , is

$${}^{Mb \cdot O_2}B_L \equiv \frac{(Mb \cdot O_2 \cdot L)}{(Mb \cdot O_2) + (Mb \cdot O_2 \cdot L)} = \frac{d \log Z_{Mb \cdot O_2}}{d \log(L)} \quad (31)$$

Returning to eq 28, we express the dependence of  $\hat{K}$  on  $(L)$  by differentiation with respect to  $\log(L)$ :

$$\begin{aligned} \frac{d \log \hat{K}}{d \log(L)} &= \frac{d \log K_0}{d \log(L)} + \frac{d \log [1 + {}^{Mb \cdot O_2}K_L(L)]}{d \log(L)} - \\ &\quad \frac{d \log [1 + {}^{Mb}K_L(L)]}{d \log(L)} \end{aligned} \quad (32)$$

Because  $K_0$  is independent of  $(L)$ ,<sup>8</sup> incorporating eqs 30 and 31 into 32, we obtain

$$\begin{aligned} \frac{d \log \hat{K}}{d \log(L)} &= {}^{Mb \cdot O_2}B_L - {}^{Mb}B_L \\ &= \nu \end{aligned} \quad (33)$$

Thus  $\nu$  can be evaluated from the dependence on  $(L)$  of the experimentally observable oxygenation equilibrium constant. Measurements of  $\hat{K}$  as a function of  $L$  reflect the binding of  $L$  to each of the species  $Mb$  and  $Mb \cdot O_2$ .

### Extension to Larger Stoichiometry for Binding of Ligand $L$

For hemoglobin, a tetrameric protein, there have been extensive studies of the effects of secondary ligands on oxygen affinity. Particular attention has been devoted to a variety of phosphates of a range of structures and sizes.<sup>9–11</sup> Direct measurements of binding of 2,3-diphosphoglycerate (DPG) have demonstrated that more than one mole of DPG is bound by hemoglobin. The effects of other phosphates on  $P_{O_2}$  suggest that they too are bound multiply. Furthermore, it has been shown<sup>12</sup> that anionic acyl salicylate is bound at several different cationic loci in hemoglobin.

Oxygen uptake by myoglobin, a monomeric protein, one-fourth the size of hemoglobin, has received far less attention

than hemoglobin. Nevertheless, there is experimental evidence that more than one auxiliary ligand can be bound by myoglobin.<sup>13</sup> It is appropriate, therefore, to extend the analysis of partitioning of ligand L to stoichiometries larger than unity.

For multiple ligand binding, the algebraic formulations must be amplified, but require no new principles. To maintain didactic concreteness, we shall focus on the partition of L between deoxymyoglobin and oxymyoglobin.

Because there is multiple binding of L in this system we write,<sup>5</sup> for Mb,

$$\left[ \begin{array}{lll} \text{Mb} + \text{L} = \text{Mb} \cdot \text{L} & K_1 = \frac{(\text{Mb} \cdot \text{L})}{(\text{Mb})(\text{L})} & (\text{Mb} \cdot \text{L}) = K_1(\text{Mb})(\text{L}) \\ \text{Mb} \cdot \text{L} + \text{L} = \text{Mb} \cdot \text{L}_2 & K_2 = \frac{(\text{Mb} \cdot \text{L}_2)}{(\text{Mb} \cdot \text{L})(\text{L})} & (\text{Mb} \cdot \text{L}_2) = K_1 K_2 (\text{Mb})(\text{L})^2 \\ \text{Mb} \cdot \text{L}_2 + \text{L} = \text{Mb} \cdot \text{L}_3; & K_3 = \frac{(\text{Mb} \cdot \text{L}_3)}{(\text{Mb} \cdot \text{L}_2)(\text{L})}; & (\text{Mb} \cdot \text{L}_3) = K_1 K_2 K_3 (\text{Mb})(\text{L})^3 \\ \vdots & \vdots & \vdots \end{array} \right] \quad (34)$$

$$\begin{aligned} (\sum \text{deoxy-Mb}) &= (\text{Mb}) + (\text{Mb} \cdot \text{L}) + (\text{Mb} \cdot \text{L}_2) + \dots \\ &= (\text{Mb})[1 + K_1(\text{L}) + K_1 K_2 (\text{L})^2 + \dots] \\ &= (\text{Mb})Z_{\text{Mb}} \end{aligned} \quad (35)$$

Correspondingly for Mb·O<sub>2</sub>,

$$\left[ \begin{array}{lll} \text{Mb} \cdot \text{O}_2 + \text{L} = \text{Mb} \cdot \text{O}_2 \cdot \text{L} & K'_1 = \frac{(\text{Mb} \cdot \text{O}_2 \cdot \text{L})}{(\text{Mb} \cdot \text{O}_2)(\text{L})} & (\text{Mb} \cdot \text{O}_2 \cdot \text{L}) = K'_1 (\text{Mb} \cdot \text{O}_2)(\text{L}) \\ \text{Mb} \cdot \text{O}_2 \cdot \text{L} + \text{L} = \text{Mb} \cdot \text{O}_2 \cdot \text{L}_2 & K'_2 = \frac{(\text{Mb} \cdot \text{O}_2 \cdot \text{L}_2)}{(\text{Mb} \cdot \text{O}_2 \cdot \text{L})(\text{L})} & (\text{Mb} \cdot \text{O}_2 \cdot \text{L}_2) = K'_1 K'_2 (\text{Mb} \cdot \text{O}_2)(\text{L})^2 \\ \vdots & \vdots & \vdots \end{array} \right] \quad (36)$$

$$\begin{aligned} (\sum \text{oxy-Mb}) &= (\text{Mb} \cdot \text{O}_2) + (\text{Mb} \cdot \text{O}_2 \cdot \text{L}) + (\text{Mb} \cdot \text{O}_2 \cdot \text{L}_2) + \dots \\ &= (\text{Mb} \cdot \text{O}_2)[1 + K'_1(\text{L}) + K'_1 K'_2 (\text{L})^2 + \dots] \\ &= (\text{Mb} \cdot \text{O}_2)Z_{\text{Mb} \cdot \text{O}_2} \end{aligned} \quad (37)$$

At any specified concentration (L), the number of moles of L bound by deoxymyoglobin,<sup>5</sup>  $^{\text{Mb}}B_{\text{L}}$ , is

$$\begin{aligned} ^{\text{Mb}}B_{\text{L}} &\equiv \frac{(\text{Mb} \cdot \text{L}) + 2(\text{Mb} \cdot \text{L}_2) + 3(\text{Mb} \cdot \text{L}_3) + \dots}{(\text{Mb}) + (\text{Mb} \cdot \text{L}) + (\text{Mb} \cdot \text{L}_2) + (\text{Mb} \cdot \text{L}_3) + \dots} \\ &= \frac{K_1(\text{L}) + 2K_1 K_2 (\text{L})^2 + 3K_1 K_2 K_3 (\text{L})^3 + \dots}{1 + K_1(\text{L}) + K_1 K_2 (\text{L})^2 + K_1 K_2 K_3 (\text{L})^3 + \dots} \\ &= \frac{d \ln Z_{\text{Mb}}}{d \ln(\text{L})} \end{aligned} \quad (38)$$

where  $Z_{\text{Mb}}$ , a partition function, is given by the denominator of the second step in eq 38. A similar set of steps for binding of L by oxymyoglobin leads to an equation for  $^{\text{Mb} \cdot \text{O}_2}B_{\text{L}}$ ,

$$^{\text{Mb} \cdot \text{O}_2}B_{\text{L}} \equiv \frac{(\text{Mb} \cdot \text{O}_2 \cdot \text{L}) + 2(\text{Mb} \cdot \text{O}_2 \cdot \text{L}_2) + \dots}{(\text{Mb} \cdot \text{O}_2) + (\text{Mb} \cdot \text{O}_2 \cdot \text{L}) + (\text{Mb} \cdot \text{O}_2 \cdot \text{L}_2) + \dots} = \frac{d \ln Z_{\text{Mb} \cdot \text{O}_2}}{d \ln(\text{L})} \quad (39)$$

In analogy to eq 33, we write

$$\begin{aligned} \nu &= ^{\text{Mb} \cdot \text{O}_2}B_{\text{L}} - ^{\text{Mb}}B_{\text{L}} \\ &= \frac{d \ln Z_{\text{Mb} \cdot \text{O}_2}}{d \ln(\text{L})} - \frac{d \ln Z_{\text{Mb}}}{d \ln(\text{L})} \end{aligned} \quad (40)$$

To obtain numerical values of  $\nu$ , we must rely on experimental data for the variation of oxygen uptake by myoglobin in solutions with varying concentration of L, but fixed pressure of O<sub>2</sub>. The observed equilibrium constant  $\hat{K}$  can be expressed as



$$\hat{K} = \frac{(\sum \text{oxy-Mb})}{(\sum \text{deoxy-Mb})(\text{O}_2)} \quad (41)$$

$$= \frac{(\text{Mb} \cdot \text{O}_2) Z_{\text{Mb} \cdot \text{O}_2}}{(\text{Mb}) Z_{\text{Mb}}} \frac{1}{(\text{O}_2)} \quad (42)$$

$$= \frac{(\text{Mb} \cdot \text{O}_2)}{(\text{Mb})(\text{O}_2)} \frac{Z_{\text{Mb} \cdot \text{O}_2}}{Z_{\text{Mb}}} \quad (43)$$

$$= K_0 \frac{Z_{\text{Mb} \cdot \text{O}_2}}{Z_{\text{Mb}}} \quad (44)$$

where  $K_0$  is the oxygenation equilibrium constant in the limit of  $(\text{L}) \rightarrow 0$ . From eq 44, it follows that

$$\log \hat{K} = \log K_0 + \log Z_{\text{Mb} \cdot \text{O}_2} - \log Z_{\text{Mb}} \quad (45)$$

Differentiating with respect to  $\log(\text{L})$  we obtain<sup>8</sup>

$$\frac{d \log \hat{K}}{d \log(\text{L})} = \frac{d \log Z_{\text{Mb} \cdot \text{O}_2}}{d \log(\text{L})} - \frac{d \log Z_{\text{Mb}}}{d \log(\text{L})} \quad (46)$$

Entering eqs 38–40, we reach the form<sup>3,4</sup>

$$\frac{d \log \hat{K}}{d \log(\text{L})} = {}^{\text{Mb} \cdot \text{O}_2} B_{\text{L}} - {}^{\text{Mb}} B_{\text{L}} = \nu \quad (47)$$

Thus a graphical presentation of experimental results for the observed  $\hat{K}$  as a function of the concentration of L (on a double-logarithmic scale) will provide  $\nu$  (as the slope of the curve at each point). From such a graph one can ascertain the partition of ligand between deoxymyoglobin and oxymyoglobin throughout the full range of concentration of ligand L.

## Conclusions

The compact stoichiometric expressions formulated for two ligands being bound to a receptor provide detailed, vivid displays of the concentration profiles for all species in coupled binding.

Such detail is not available in analyses centering on inter-relationships between binding constants. Full analytic details have been presented here for the simplest case, each of two ligands bound with unit stoichiometry to receptor. For multiple binding of the auxiliary ligand L, the appropriate algebraic approach is described and the equation showing partitioning of L between receptor species is explicitly derived.

Our analytic format, described in terms of protein–ligand interactions, is also applicable to other interacting systems, including those of macromolecular assembly.<sup>4</sup> For example, duplex–single strand equilibria of oligonucleotides are very sensitive to concentrations of auxiliary ligands L. Concentration profiles for the macromolecular species in these equilibria can also be defined and computed by the algebraic approaches described here.

## References and Notes

- (1) Gibbs, J. W. *Trans. Conn. Acad. Sci.* **1876**, 3, 108; **1878**, 3, 343.
- (2) Bohr, C.; Hasselbalch, K. A.; Krogh, A. *Skand. Arch. Physiol.* **1904**, 16, 401.
- (3) Wyman, J. *Adv. Protein Chem.* **1964**, 19, 223.
- (4) Wyman, J.; Gill, S. J. *Binding and Linkage: Functional Chemistry of Biological Macromolecules*; University Science Books: Mill Valley, CA, 1990.
- (5) Klotz, I. M. *Ligand–Receptor Energetics*; John Wiley and Sons: New York, 1997.
- (6) Rossi Fanelli, A.; Antonini, E. *Arch. Biochem. Biophys.* **1958**, 77, 478.
- (7) A complete set of curves is available at <http://www.ligandBinding.org> or can be obtained by request to Dr. Isard Dunietz (idunietz@idtdna.com) at Integrated DNA Technologies, Inc.
- (8) It is implicitly assumed that any variation of  $\log K_0$  with L due to secondary interactions (e.g., Debye–Hückel ionic effects) may be neglected.
- (9) Chanutin, A.; Curnish, R. R. *Arch. Biochem. Biophys.* **1967**, 121, 96.
- (10) Benesch, R.; Benesch, R. E. *Biochem. Biophys. Res. Commun.* **1967**, 26, 162.
- (11) Benesch, R.; Benesch, R. E. *Proc. Natl. Acad. Sci. U.S.A.* **1968**, 59, 526.
- (12) Shamsuddin, M.; Mason, R. G.; Ritchey, J. M.; Honig, G. R.; Klotz, I. M. *Proc. Natl. Acad. Sci. U.S.A.* **1974**, 71, 4693.
- (13) Antonini, E.; Brunori, M. *Hemoglobin and Myoglobin in their Reactions with Ligands*; North-Holland Publishing Co.: Amsterdam, 1971.